

Determination of the differences between the charge radii of zirconium nuclei using laser-excited resonance fluorescence

Yu. P. Gangrskii, S. G. Zemlyanoi, B. K. Kul'dzhanov,¹⁾ K. P. Marinova, B. N. Markov, Hoang Thi Kim Hue, and Chan Kong Tam

Joint Institute for Nuclear Research, Dubna

(Submitted 3 November 1987)

Zh. Eksp. Teor. Fiz. **94**, 9–18 (June 1988)

The optical isotopic shifts of all the stable zirconium isotopes were determined for three atomic transitions of the $4d^2 5s^2 \rightarrow 4d^2 5s 5p$ type by the method of laser-excited resonance fluorescence. The differences between the mean-square charge radii $\Delta \langle r^2 \rangle$ were determined for zirconium ions. A comparison of the values of $\Delta \langle r^2 \rangle$ obtained in this way with the predictions of the liquid drop model demonstrated that the calculations were in agreement with the experimental results provided an allowance was made for the dynamic octupole deformation of the nuclei and for the thickness of the surface layer.

1. INTRODUCTION

Determination of the differences between the mean-square charge radii of the nuclei of the adjacent isotopes provides a rich source of important information on the properties of atomic nuclei. This information can be used to judge the effective interactions of the nucleons in the nuclei and to estimate the values of a whole range of nuclear parameters such as deformation of the nuclei, thickness of the surface layer, and magnitudes of the pair correlations. It is usual to assume that the change in the charge radius with the number of neutrons in a nucleus depends, in the first approximation, on two main factors.

1. The first factor is the increase in the volume of the nucleus, which is determined by the number of nucleons inside it. For small changes in the mass number A the difference between the mean-square charge nuclei is

$$\Delta \langle r^2 \rangle_v = 0.576 \chi \Delta A / \bar{A}^3, \quad (1)$$

where χ is an empirical parameter (its value is 0.5–0.7) representing the following relationship: when only the number of neutrons in a nucleus is altered, its charge radius rises more slowly than would follow from the dependence $\gamma \propto A^{1/3}$. This is explained either by the compressibility of the nuclei¹ or by the hypothesis that the other nuclei are not distributed throughout the volume of the nucleus, but are concentrated preferentially in its surface layer.²

2. The other factor is the deformation of a nucleus which may be static and determine its shape, or dynamic and associated with fluctuations of its surface. The corresponding dependence is

$$\Delta \langle r^2 \rangle_\beta = 0.344 \bar{A}^3 \sum_i \Delta (\beta_i^2), \quad (2)$$

where β_i are the deformation parameters of different orders (quadrupole, octupole, etc.).

In the case of the majority of the investigated isotope chains the variation of the mean-square charge radii is practically entirely due to the above two factors: distortions due to the deformation of a nucleus are superimposed on a smooth dependence of the mean-square charge radius of a nucleus on the number of neutrons inside it. In the case of some chains the influence of deformation is so strong that the mean-square charge radii begin to increase when the number of neutrons is reduced, for example, in the case of

neutron-deficient isotopes of Rb (Ref. 3) and Sr (Ref. 4).

However, in the case of some nuclei there are other factors that influence the mean-square charge radii. They include the nuclei of Kr (Ref. 5) and Sr (Ref. 6) near the closed shell of 80 neutrons, as well as Nd, Sm, and Gd (Ref. 7) in the region of $N = 90$. This may be due to a change in the thickness of the surface layer in a nucleus. More reliable conclusions and numerical estimates of the thickness of the surface layer require accurate allowance for the influence of the deformation of a nucleus. However, in most cases this is difficult because the values of the deformation parameters are not known very accurately. In this respect the isotopes of zirconium with the number of neutrons close to 50 have certain advantages because the closed subshell of 40 protons also has a stabilizing influence on the shape of the nucleus. The value of the quadrupole moment of the ^{91}Zr nucleus ($Q = 0.21$ b—see Ref. 8) yields the static quadrupole deformation parameter $\beta_2 \sim 0.07$ and the dynamic deformation parameter calculated from the reduced probabilities of electric quadrupole transitions in even–even nuclei is $\langle \beta^2 \rangle^{1/2} \leq 0.1$ (Ref. 9). Therefore, the contribution of the deformation to the change in the mean-square charge radii is small and this makes it possible to determine the influence of other factors on these radii.

The system of energy levels of neutral zirconium atoms with configurations of the $(4d + 5s)^4$ type consists of a large number of low-lying and closely spaced levels, which interact with one another.¹⁰ This makes it difficult to determine the differences between the charge nuclei from the measured isotopic shifts. One should add here the difficulties encountered in the generation of sufficiently intense atomic beams because of the high melting point (1850 °C) and the low saturated vapor pressure of zirconium (for example, this pressure is 10^{-3} Torr at 2170 °C). This is clearly the reason why the absolute values of the differences between the charge radii of zirconium nuclei have not yet been obtained from measurements of optical spectra. In Ref. 11, reporting a study carried out by the classical interference technique, there are only data on the relative values of the mean-square charge nuclei and the work based on laser spectroscopy (see, for example, Refs. 12 and 13) has been limited to determination of the isotopic shift of the even–even zirconium isotopes. Moreover, x-ray spectra of zirconium have not yet been determined and the spectra of muonic atoms have

yielded only the difference between the mean-square charge nuclei for one pair of isotopes ^{90}Zr and ^{92}Zr , for which we have $\Delta\langle r^2 \rangle^{90,92} = 0.306 \text{ fm}^2 \text{ C}$ (Ref. 14).

2. EXPERIMENTAL METHOD

We used the method of laser-excited fluorescence. The laser radiation frequency could be varied by up to 30 GHz and the laser beam crossed a collimated atomic beam. The resonance fluorescence excited in this way was detected with a photomultiplier operating in the single-photon counting mode. The laser radiation, the atomic beam, and the direction of detection fluorescence were mutually perpendicular. The apparatus was described and its parameters were given in Refs. 15 and 16.

In the present study we used a modification of that apparatus: instead of evaporation of the investigated sample from an electrically heated crucible, the atomic beam was formed by laser evaporation. We used the setup represented by a block diagram in Fig. 1. An optical system was used to focus pulses from an LTIPC-7 YAG laser type ($\lambda = 1.06 \mu\text{m}$, pulse duration $\tau_p = 10 \text{ ns}$, pulse repetition frequency 10–100 Hz, output power 8 MW) on the surface of a sample. A photomultiplier (PM in Fig. 1) signal passed along a fast electronic channel (amplifier, discriminator, gate) and was recorded with a multichannel analyzer operating in the time mode and synchronized with variation of the wavelength of the exciting cw laser. A suitable selection of the power density of the radiation from the pulsed laser, of the delay in counting the photomultiplier signals relative to the laser pulse, and of the delay in opening of the gate established optimal operating conditions. Laser evaporation was found to be a convenient atomization method, which made it possible to observe resonant excitation of atoms of all the zirconium isotopes with a sufficiently high yield of the fluorescence. We used metal zirconium samples with the natural isotopic composition and zirconium oxide (ZrO_2) samples enriched with the ^{91}Zr isotope to 90%.

The half-width of the resonance fluorescence line was governed by the Doppler broadening of the atomic beam and amounted to 45 MHz (the half-width of the line emitted by a dye laser with an active stabilization unit was $\sim 3 \text{ MHz}$). This made it possible to distinguish reliably those peaks in the optical spectrum which corresponded to all the even isotopes of zirconium and to the hyperfine structure components of the Zr odd isotope. The nonlinearity of the laser frequency tuning was allowed for by recording timing marks in the analyzer simultaneously with the optical spectra; these marks were generated using a confocal Fabry-Perot interferometer with a time constant 150 MHz.

3. EXPERIMENTAL RESULTS

Table I shows the parameters of the optical transitions in zirconium: the wavelengths, the terms, the configurations

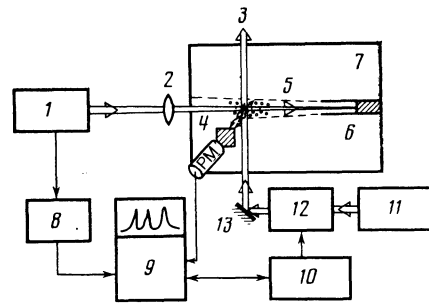


FIG. 1. Block diagram of the apparatus with laser evaporation: 1) pulsed evaporation laser; 2) lens; 3) beam of cw tunable laser; 4) filter; 5) gate generator; 6) crucible with sample; 7) chamber; 8) atomic beam; 9) analyzer with a microprocessor; 10) tuning unit; 11) argon laser; 12) cw dye laser; 13) mirror.

and the energies of the initial and final states,¹⁷ for which the isotopic shifts were measured.

Figure 2a shows the recorded spectrum of a sample of natural composition, whereas Fig. 2b is the hyperfine structure spectrum of a sample enriched with ^{91}Zr . In the latter case we resolved all nine components of the transition. This made it possible to identify the hyperfine structure components allowing for the familiar hyperfine splitting of the lower level.⁸ Figure 2b shows this identification: F is the total momentum of the lower level and F' is the corresponding momentum of the upper level. The method used in determination of the isotopic shift of the center of gravity (c.g. in Fig. 2b) of the hyperfine structure of the ^{91}Zr odd isotope relative to the neighboring even-even isotope was described by us in Ref. 18. The experimental values of the isotopic shifts are listed in Table II for all the investigated optical lines together with the error of a single measurement.

The consistency of the isotopic shifts was checked using a King graph^{19,20}:

$$y_i^{A,A'} = \frac{E_i}{E_j} y_j^{A,A'} + \left(M_i - M_j \frac{E_i}{E_j} \right) \frac{A_0' - A_0}{A_0 A_0'}, \quad (3)$$

where $y^{A,A'}$ are the modified isotopic shifts for the pair of the optical transitions i and j being compared, characterized by $A_0 = 90$ and $A_0' = 92$ (mass numbers of the zirconium isotopes),

$$y^{A,A'} = \Delta v_{\text{exp}}^{A,A'} \frac{AA'}{A' - A} \frac{A_0' - A_0}{A_0 A_0'}, \quad (4)$$

M are constants typical of a given transition and related to the mass isotopic shifts:

$$\Delta v_{\text{MS}}^{A,A'} = M \frac{A' - A}{AA'}, \quad (5)$$

and E is the electron factor (discussed below). In all cases the King graph was calculated by the least-squares method (LSM) allowing for the random errors of both the lines be-

TABLE 1. Characteristics of optical transitions in zirconium.

$\lambda, \text{\AA}$	Term	Configuration	Energy, cm^{-1}
5735.70	$a^3F_2 \rightarrow z^3D_1^0$	$4d^25s^2 \rightarrow 4d^25s5p$	$0 \rightarrow 17\,429.86$
5797.74	$a^3F_3 \rightarrow z^3D_2^0$	$4d^25s^2 \rightarrow 4d^25s5p$	$570.41 \rightarrow 17\,813.64$
5885.62	$a^3F_3 \rightarrow z^3F_4^0$	$4d^25s^2 \rightarrow 4d^25s5p$	$570.41 \rightarrow 17\,556.26$

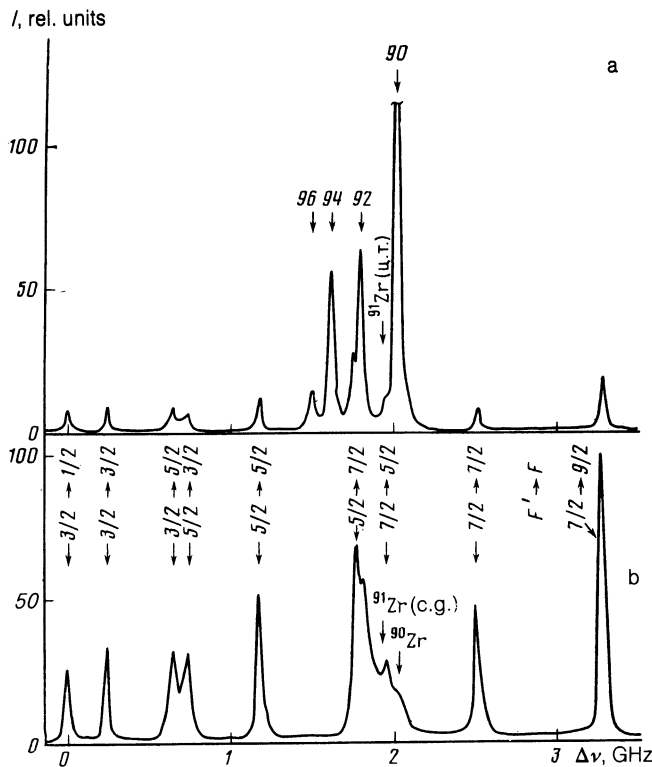


FIG. 2. Resonance fluorescence spectrum of zirconium obtained for the $4d^2 5s^2 \ ^3F_2 \rightarrow 4d^2 5s 5p^3 \ ^3D_1^0$ transition at the frequency $\lambda = 5735.70 \text{ \AA}$: a) sample with natural isotopic composition; b) hyperfine structure of ^{91}Zr obtained for an enriched sample of $^{91}\text{ZrO}_2$.

ing compared. The deviations of the experimental values from the King line, i.e., the quantities $\Delta y_i^{A,A'} = y_{i,\text{exp}}^{A,A'} - y_{i,\text{LSM}}^{A,A'}$, are plotted in Fig. 3 as a function of the modified isotopic shift of the reference line ($\lambda = 5735.70 \text{ \AA}$). It is clear that the compatibility of our measurements was very good. A similar comparison was also made for the $\lambda = 5935.20 \text{ \AA}$ transition^{12,13} investigated by laser spectroscopy, and for the $\lambda = 4687.80 \text{ \AA}$ transition studied by the classical interference method.¹¹ In the latter case the deviations $\Delta y_i^{A,A'}$ were large.

4. DETERMINATION OF THE DIFFERENCES BETWEEN THE MEAN-SQUARE CHARGE RADII

The difference between the mean-square charge radii ($\Delta \langle r^2 \rangle$) was determined by a standard procedure described in Refs. 7 and 21. In the calculation of $\Delta \langle r^2 \rangle$ it was necessary to carry out the following procedures: 1) using the experimental isotopic shifts, to calculate the total isotopic shift

consisting of the normal mass shift $\Delta \nu_{\text{NMS}}$ and the specific mass shift $\Delta \nu_{\text{SMS}}$; 2) to calculate the electron factor E_i governing the change in the nonrelativistic density of the electron charge $\Delta |\psi(0)|^2$ at the position of the nucleus for the transition under investigation (i); 3) to determine the nuclear factor $f(Z)$ governing the corrections to the electron wave function because of the relativistic effects and finite size of the nucleus.

It is clear from Table I that all the transitions we investigated were of the $ns^2 \rightarrow nsnp$ type. In the case of pure transitions of this type a specific mass shift was found to be described by the expression²¹

$$\Delta \nu_{\text{SMS}}^{A,A'} = (0 \pm 0.5) \Delta \nu_{\text{NMS}}^{A,A'} \quad (6)$$

However, in our case there might be mixing of the configurations of the states. This was supported by the differences between the theoretical and experimental values of the g factors of the levels and by the deviations from the Landé interval rules for multiplet splittings.¹⁷

Therefore, the values of $\Delta \nu_{\text{SMS}}$ for the investigated transitions in zirconium were deduced from the known value of $\Delta \nu_{\text{SMS}}$ for the $4d^3 5s a^5 F_5 \rightarrow 4d^3 5p y^5 G_6^0$ transition characterized by $\lambda = 4687.8 \text{ \AA}$ (Ref. 11) using the above-mentioned King graph.^{19,20} It was assumed that the latter transition was a pure alkali-like transition of the $ns \rightarrow np$ type for which the theoretical estimates gave²¹

$$\Delta \nu_{\text{SMS}}^{A,A'} = (0.3 \pm 0.9) \Delta \nu_{\text{NMS}}^{A,A'} \quad (7)$$

The King graph (Fig. 4) was plotted so that the ordinate represented the values of the modified isotopic shift of the reference line with $\lambda = 4687.80 \text{ \AA}$ ($\Delta \nu_{\text{ex}} - \Delta \nu_{\text{NMS}}$), whereas the abscissa represented the modified experimental values of the isotopic shift of the investigated lines. In this case the point of intersection of the King line with the abscissa gave the mass shift of the investigated line. In these calculations we allowed for the random errors of all the lines and the theoretical error in $\Delta \nu_{\text{SMS}}$ of the reference line. The values of $\Delta \nu_{\text{SMS}}$ obtained in this way are listed in Table III. The large errors in the values of $\Delta \nu_{\text{SMS}}$ were due to the indeterminacy of the theoretical estimate $\Delta \nu_{\text{SMS}}$ of the reference line and the relatively large errors in the experimental values of the isotopic shifts for the same line (Fig. 4). These errors prevented us from judging reliably the purity of the configurations of the states.

The configuration mixing prevented us from accurate calculations of the electron factor E_j for the investigated transitions. Therefore, E_j was determined from the slope of the King line [Eq. (3)]: E_i/E_j , where E_i is the electron factor of the reference line with $\lambda = 4687.80 \text{ \AA}$. In the case of the pure $ns \rightarrow np$ transition, the electron factor was

TABLE II. Experimental values of the isotopic shifts of zirconium deduced from different optical transitions: $\Delta \nu_{\text{exp}}^{A,A'} = \nu^{A'} - \nu^A$, MHz.

A	A'	$\lambda = 5735.70 \text{ \AA}$	$\lambda = 5797.74 \text{ \AA}$	$\lambda = 5885.62 \text{ \AA}$
90	92	-237 (2)	-222 (2)	-226 (1)
90	91	-97 (7)	-93 (4)	-
92	94	-172 (4)	-163 (2)	-168 (1)
94	96	-115 (3)	-97 (2)	-115 (2)

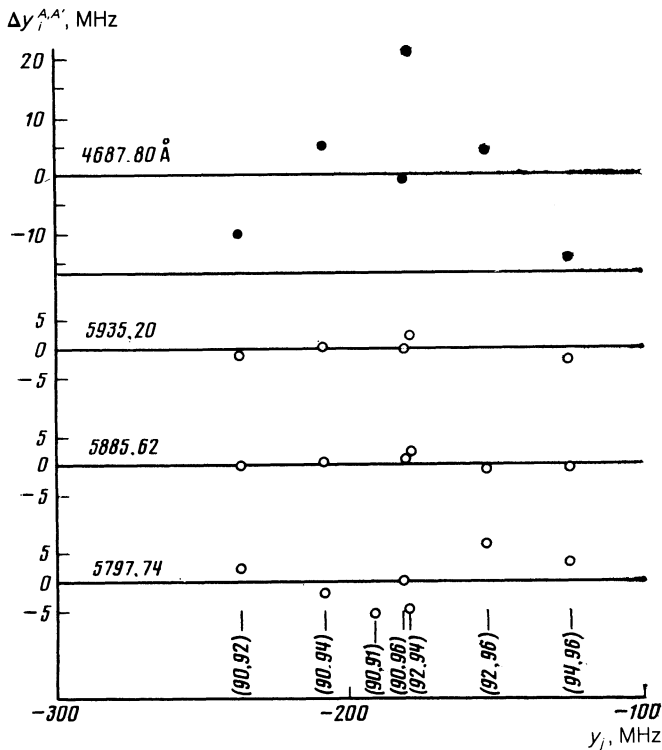


FIG. 3. Deviations of the experimental values of $\Delta y_i^{A,A'}$ of the modified isotopic shift, deduced for different optical transitions from the King line determined by the least-squares method. Here, $y_i^{A,A'} = \Delta v_{\text{exp}}^{A,A'}$ ($\lambda = 5735.70 \text{ \AA}$) $[AA'/A' - A](2/90 \times 92)$.

$$E_i = E_{ns \rightarrow np} = -\beta \frac{\pi a_0^3}{Z} |\psi(0)|_{ns}^2, \quad (8)$$

where Z is the atomic number of the element, a_0 is the Bohr radius, $|\psi(0)|_{ns}^2$ is the density of the electron charge at the position of the nucleus in the case of the ns atomic configuration, and β is the screening parameter. According to Ref. 11, in the Goudsmit-Fermi-Segré approximation we have $|\Psi(0)|_{ns}^2 = 1/2.72$ (in units of $Z/\pi a_0^3$). Nonrelativistic calculations carried out by the Hartree-Fock method²² indicate that in the case of pure $4d^{35}5^5F \rightarrow 4d^{35}5p$ transitions in zirconium the screening parameter is $\beta = 1.23$. Substitution of all the relevant values in Eq. (8) gives $E_i = -0.452$. The values of the slope E_i/E_j and of the electron factor E_j are listed in Table III. The error given for the electron factor includes the error in the slope of the King line and the error in E_i of the reference line, estimated to be about 5%.

The value of the nuclear factor $f(Z)$ for the $^{90,92}\text{Zr}$ isotope pair is also included in Table III. The calculations were carried out using the familiar expression given in Ref. 23.

TABLE III. Parameters used in calculations of $\Delta \langle r^2 \rangle$ ($A = 90, A' = 92$).

$\lambda, \text{ \AA}$	$\Delta v_{\text{NMS}}, \text{ MHz}$	$\Delta v_{\text{SMS}}, \text{ MHz}$	$\Delta v_{\text{PS}}, \text{ MHz}$	E_i/E_j	E_j	$f(Z), \text{ GHz/fm}^2$
5735.70	69.3	-50 (40)	-260 (40)	1.80 (13)	-0.252 (22)	4.475
5797.74	68.5	-20 (50)	-270 (50)	1.64 (15)	-0.276 (28)	4.475
5885.62	67.5	-60 (40)	-240 (40)	1.94 (14)	-0.233 (21)	4.475

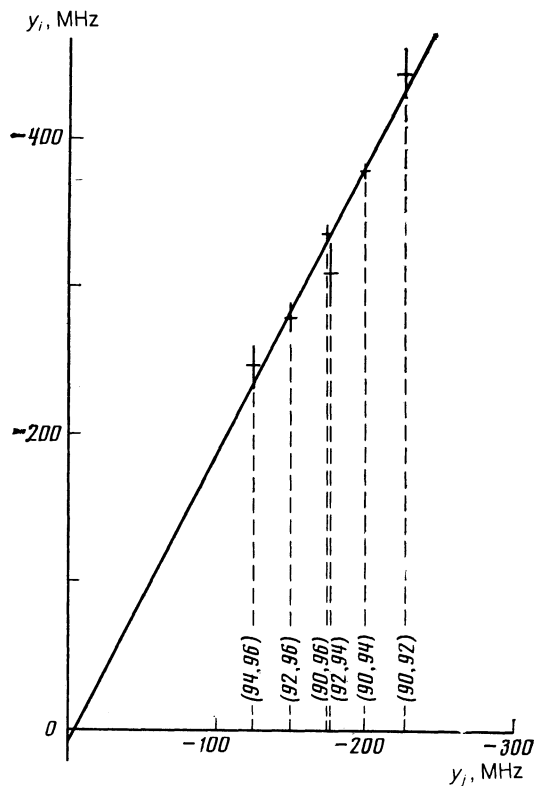


FIG. 4. Example of a King graph used in the experimental determination of the specific mass shift and of the electron factor of the investigated transitions. Here, $y_i^{A,A'} = y_{\text{exp}}^{A,A'} - y_{i,\text{NMS}}^{A,A'}$ for $\lambda = 4687.80 \text{ \AA}$. The triple statistical errors are shown.

The calculations were carried out using the mean-square charge radius $\langle r^2 \rangle^{1/2} = 4.266(14) \text{ fm}$ (Ref. 24) and the theoretical isotopic shift constant for a singly charged sphere with $C^{90,92} = 37.5 \text{ mK}$ allowing for the relativistic correction.²⁵

The experimental isotopic shifts (Table II) and the parameters listed in Table III were used to find the relative and absolute values of the differences between the mean-square charge radii of the zirconium isotope pairs (Table IV) using a calculation procedure we described in Ref. 7. It is clear from this table that in the case of the $^{90,92}\text{Zr}$ isotope pair the value of $\Delta \langle r^2 \rangle$ was much less than for the same pair deduced from the spectrum of muonic atoms.¹⁴

For comparison, we included in Table IV the values of $\Delta \langle r^2 \rangle^{A,A+2}$ for the molybdenum nuclei with the same number of neutrons.²⁶ The agreement was good for the nuclei with $N = 50-54$. In the case of the $^{90,91}\text{Zr}$ pair of nuclei, differing by one neutron the value of $\Delta \langle r^2 \rangle$ was close to half the

TABLE IV. Relative $\lambda_{rel}^{A,A'}$ and absolute $\Delta\langle r^2 \rangle$ values for zirconium isotopes and absolute changes in the mean-square radii of molybdenum.

Zr				Mo		
A	A'	$\lambda_{rel}^{A,A'}$	$\Delta\langle r^2 \rangle, \text{fm}^2$	A	A'	$\Delta\langle r^2 \rangle, \text{fm}^2$
90	92	1.000	0.224 (25)	92	94	0.226 (19)
90	91	0.429 (16)	0.096 (11)			
92	94	0.759 (21)	0.170 (19)	94	96	0.193 (16)
94	96	0.52 (4)	0.117 (14)	96	98	0.150 (12)

corresponding value of $\Delta\langle r^2 \rangle$ on addition of a pair of neutrons (^{90}Zr and ^{92}Zr nuclei). This was an indication of small even-odd differences between the mean-square charge radii of the zirconium nuclei.

5. DISCUSSION OF RESULTS

Figure 5 shows how the difference between mean-square radii of the adjacent even-even isotopes depends on the number of neutrons in the nucleus. For comparison, we included the results of calculations obtained by applying the simple empirical dependence $\gamma^2 \propto A^{2/3}$ (line 1) and that deduced from the liquid drop model²⁷ using the parameters from Ref. 28 (line 2). In the latter case the calculations were made for a constant value of the surface diffuseness parameter b amounting to 0.946 fm (representing the experimental value for ^{90}Zr).²⁹ There was a considerable difference: both calculations predicted a weak dependence of the values of $\Delta\langle r^2 \rangle$ on the number of neutrons in the nucleus, whereas the experimental values fell by a factor of two on transition from the (90, 92) pair of isotopes to the (94, 96) pair.

As pointed out above, such behavior of the differences between the mean-square charge nuclei can be attributed to a change in the nuclear deformation. It is assumed that the shape of the zirconium nuclei is nearly spherical and that the dominant influence on the shape is the dynamic deformation due to the quadrupole vibrations of the nuclear surface. The values of the quadrupole deformation parameters⁹ and the corresponding differences between the mean-square charge radii $\Delta\langle r^2 \rangle$ deduced from Eq. (2) are listed in Table V. We can see that these values of $\Delta\langle r^2 \rangle$ are small (smaller than the error in the determination of $\Delta\langle r^2 \rangle$) and their inclusion can-

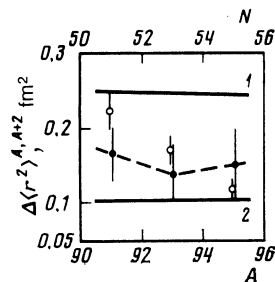


FIG. 5. Dependences of the difference between the charge radii of the adjacent even-even zirconium isotopes on the mass number A : 1) values of $\Delta\langle r^2 \rangle$ calculated from the empirical dependence $r^2 \propto A^{2/3}$; 2) values of $\Delta\langle r^2 \rangle_{DM}$ calculated using the drop model; (●) values calculated from Eq. (9); (○) experimental values of $\Delta\langle r^2 \rangle$.

not account for the observed dependence of $\Delta\langle r^2 \rangle$ on the number of neutrons in the nucleus.

Clearly, we have to allow for deformations of higher orders, particularly for the dynamic octupole deformation. The values of the parameters of this deformation (β_3) for the zirconium nuclei can be deduced from experiments on inelastic scattering of charged particles (a summary of the data is given in Refs. 30 and 31). Although the values deduced from experiments carried out employing different particles with different energies differed somewhat, the general trend of variation of β_3 was the same: the values of β_3 increased on increase in the number of neutrons in a nucleus. The average values of β_3 are listed in Table V. We can see that they are much larger than the parameters of the quadrupole deformation and consequently give rise to larger values of $\Delta\langle r^2 \rangle_{\beta_3}$.

We can see from Fig. 5 that inclusion of the corrections associated with both types of deformation (β_2, β_3), i.e., the quantity deduced from the drop model (DM)

$$\Delta\langle r^2 \rangle_{DM} + \sum_{i=2,3} \Delta\langle r^2 \rangle_{\beta_i}, \quad (9)$$

gives a better agreement between the values of $\Delta\langle r^2 \rangle$ calculated from the drop model and the experimental data. Inclusion of deformation of the next order (hexadecapole β_4) may improve still further the agreement between the calculated and experimental values. However, the values of β_4 for zirconium nuclei are not known.

Calculations carried out using the drop model with a suitable allowance for the quadrupole and the octupole deformations can be matched to the experimental values of $\Delta\langle r^2 \rangle$ if we allow for possible changes in the thickness of the surface layer in the distribution of the charge in the nuclei. Since such changes are described by the parameter b , the results can be matched by altering the value of b for different isotopes (retaining $b = 0.946$ fm for ^{90}Zr). The values of b found in this way are listed in Table V. We can see that even the largest discrepancy between the experimental and calculated values (the latter corrected for the deformation) of the changes in the mean-square charge radii, amounting to 0.056 fm² for the $^{90,92}\text{Zr}$ pair (Fig. 5), can be eliminated by altering b for ^{92}Zr by just 1%.

It therefore follows that the observed values of the differences between the mean-square charge radii for the zirconium nuclei and their dependence on the number of neutrons in the nucleus can be explained provided we bear in mind the changes in the dynamic octupole deformation of the nuclei and in the thickness of the surface layer.

TABLE V. parameters of deformation of zirconium nuclei and corresponding differences between mean-square charge radii and parameters of the surface layer.

A	Quadrupole vibrations		Octupole vibrations		b, fm
	β_2	$\Delta\langle r^2 \rangle_{\beta_2}^{A, A+2}, \text{fm}^2$	β_3	$\Delta\langle r^2 \rangle_{\beta_3}^{A, A+2}, \text{fm}^2$	
90	0.091 (4)	0.016 (17)	0.15 (1)	0.04 (3)	0.946 *
92	0.104 (4)	-0.017 (14)	0.17 (1)	0.05 (4)	0.955 (7)
94	0.090 (10)	-0.011 (22)	0.19 (1)	0.06 (4)	0.960 (10)
96	0.086 (16)		0.21 (1)		0.955 (13)

*Taken from Ref. 29 with a correction for the deformation.

The authors are grateful to G. N. Flerov and Yu. Ts. Oganessian for their encouragement, to B. B. Krynetskiĭ and S. K. Borisov for valuable discussions, to N. B. Buyanov for his help in the alignment of the laser spectrometer, and to G. V. Myshinskiĭ for his help in the experiments.

¹Institute of Nuclear Physics, Academy of Sciences of the Uzbek SSR.

¹E. W. Otten, *Hyperfine Interactions* **2**, 127 (1976).

²W. D. Myers, *Phys. Lett. B* **30**, 481 (1969).

³C. Thibault, F. Touchard, S. Büttgenbach, R. Klapisch, M. de Saint Simon, H. T. Duong, P. Jacquinet, P. Juncar, S. Liberman, P. Pillet, J. Pinard, J. L. Vialle, A. Pesnelle, and G. Huber, *Phys. Rev. C* **23**, 2720 (1981).

⁴D. A. Eastham, P. M. Walker, J. R. H. Smith, D. D. Warner, J. A. R. Griffith, D. E. Evans, S. A. Wells, M. J. Fawcett, and I. S. Grant, *Phys. Rev.* **36**, 1383 (1987).

⁵H. Gerhardt, E. Matthias, H. Rinneberg, F. Schneider, A. Timmermann, R. Wenz, and P. J. West, *Z. Phys. A* **292**, 7 (1979).

⁶A. G. Martin, S. B. Dutta, W. F. Rogers, and D. L. Clark, *Phys. Rev. C* **34**, 1120 (1986).

⁷S. K. Borisov, Yu. P. Gangrskii, Ch. Gradechny, S. G. Zemlyanov, B. B. Krynetskiĭ, K. P. Marinova, B. N. Markov, V. A. Mishin, Yu. Ts. Oganessian, O. M. Stel'makh, Hoang Thi Kim Hue, and Chan Kong Tam, *Zh. Eksp. Teor. Fiz.* **93**, 1548 (1987) [*Sov. Phys. JETP* **66**, 882 (1987)].

⁸S. Büttgenbach, R. Dicke, H. Gebauer, R. Kuhnen, and F. Träber, *Z. Phys. A* **286**, 128 (1978).

⁹S. Raman, C. H. Malarkey, W. T. Milner, C. W. Nestor Jr., and P. H. Stelson *At. Data Nucl. Data Tables* **36**, 1 (1987).

¹⁰S. Büttgenbach, R. Dicke, and H. Gebauer, *Phys. Lett. A* **58**, 86 (1976).

¹¹K. Heilig, K. Schmitz, and A. Steudel, *Z. Phys.* **176**, 120 (1963).

¹²O. L. Bourne, M. R. Humphries, S. A. Mitchell, and P. A. Hackett, *Opt. Commun.* **56**, 403 (1986).

¹³G. Chevalier and J. M. Gagne, *Opt. Commun.* **57**, 327 (1986).

¹⁴R. Engfer, H. Schneuwly, J. L. Vuilleumier, H. K. Walter, and H. Zehnder, *At. Data Nucl. Data Tables* **14**, 809 (1974).

¹⁵Yu. P. Gangrskii, K. P. Marinova, B. N. Markov, E. G. Nadzhakov, Yu. Ts. Oganessian, Han Gen Yi, and Chan Kong Tam, *Izv. Akad. Nauk SSSR Ser. Fiz.* **49**, 2261 (1985).

¹⁶Yu. P. Gangrskiy, Han Gen Yi, K. P. Marinova, *et al.*, Preprint No. E6-86-233, Joint Institute for Nuclear Research, Dubna (1986).

¹⁷C. E. Moore, *Atomic Energy Levels as Derived from the Analyses of Optical Spectra*, Vol. 2, National Bureau of Standards, Washington, D.C. (1952) [NBS Circ. No. 467].

¹⁸Yu. P. Gangrskii, S. G. Zemlyanoi, B. K. Kul'dzhanov, *et al.*, preprint No. R6-87-478 [in Russian], Joint Institute for Nuclear Research, Dubna (1987).

¹⁹W. H. King Jr., *J. Opt. Soc. Am.* **53**, 638 (1963).

²⁰J. Bauche and R. J. Champeau, in: *Advances in Atomic and Molecular Physics* (ed. by D.R. Bates and B. Bederson), Vol. 12, Academic Press, New York (1976), p. 39.

²¹K. Heilig and A. Steudel, *At. Data Nucl. Data Tables* **14**, 613 (1974).

²²P. Aufmuth, *J. Phys. B* **15**, 3127 (1982).

²³F. A. Babushkin, *Zh. Eksp. Teor. Fiz.* **44**, 1661 (1963) [*Sov. Phys. JETP* **17**, 1118 (1963)].

²⁴E. Wesolowski, *J. Phys. G* **10**, 321 (1984).

²⁵D. Zimmermann, *Z. Phys. A* **315**, 123 (1984).

²⁶P. Aufmuth, H. P. Clieves, K. Heilig, A. Studel, D. Wendlandt, and J. Bauche, *Z. Phys. A* **285**, 387 (1978).

²⁷W. D. Myers and W. J. Swiatecki, *Nucl. Phys. A* **336**, 267 (1980).

²⁸W. D. Myers and K. H. Schmidt, *Nucl. Phys. A* **410**, 61 (1983).

²⁹J. Friedrich and N. Voegler, *Nucl. Phys. A* **373**, 192 (1982).

³⁰M. Lahanas, D. Rychel, P. Singh, R. Gyufko, D. Kolbert, B. van Kruchten, E. Madadakis, and C. A. Wiedner, *Nucl. Phys. A* **485**, 399 (1986).

³¹p. Singh, D. Rychel, R. Gyufko, B. van Kruchten, M. Lahanas, and C. A. Wiedner, *Nucl. Phys. A* **458**, 1 (1986).

Translated by A. Tybulewicz